Environ Geol (2007) 51: 775–779
DOI 10.1007/s00254-006-0394-y

ORIGINAL ARTICLE

Douchko Romanov
Franci Gabrovsek
Wolfgang Dreybrodt

Leakage below dam sites in limestone terrains by enhanced karstification: a modeling approach

Received: 9 October 2005
Accepted: 23 May 2006
Published online: 22 August 2006

D. Romanov (✉) · W. Dreybrodt
Department of Earth Sciences,
Freie Universität Berlin,
Berlin, Germany
E-mail: dromanov@zedat.fu-berlin.de
E-mail: dreybrodt@ifp.uni-bremen.de

F. Gabrovsek
Karst Research Institute ZRC SAZU,
Postojna, Slovenia
E-mail: gabrovsek@zrc-sazu.si

Abstract Unnaturally high hydraulic gradients below dam sites enhance dissolutional widening of fractures in limestone. A model is presented which suggests that under unfavorable conditions, leakage rates could become unbearably high during the lifetime of the dam. At the beginning when water is impounded, leakage rates are low and increase slowly. A positive feedback loop, however, causes a sudden dramatic increase of leakage within a few years. Deep grouting becomes necessary to prevent such failures. Inefficiencies in grouting may leave some open fractures in the grouting curtain. These fractures widen faster than pathways below the grouting curtain, and reduce the effect of the grouted region located below. Therefore, open fractures act in a similar way as reduction of the grouting depth.

Keywords Dissolution of limestone · Karstification · Dam site

Introduction

Water flowing through narrow fissures and fractures in soluble rock, such as limestone and gypsum, widens these by chemical dissolution. Close to saturation, characteristic non-linear dissolution kinetics cause a feedback mechanism, giving rise to a breakthrough behavior of the flow rates. If constant head h drives flow of aggressive water through a single fracture of aperture width a_0 and length L, initially flow rates increase slowly, but then suddenly at breakthrough time T they increase dramatically. The breakthrough time can be derived by mathematical analysis (Dreybrodt 1996; Dreybrodt and Gabrovsek 2003). It is given by

$$T \infty \left(\frac{L^2}{h}\right)^{\frac{n}{n-1}} \cdot a_0^{\frac{2n+1}{n-1}} \cdot k_n^{\frac{1}{n-1}} \cdot c_{\mathrm{eq}}^{\frac{-n}{n-1}}. \quad (1)$$

The constants n, k_n, and c_{eq} characterize the dissolution rates close to equilibrium (Eisenlohr et al 1999; Jeschke et al. 2001), which are given by

$$R = k_n(1 - c/c_{\mathrm{eq}})^n, \quad n \approx 4, \quad c \geq 0.9c_{\mathrm{eq}} \quad (2)$$

c_{eq} is the equilibrium concentration of calcium. For karstification under natural conditions, with $L \approx 10$ km and $h \approx 100$ m, breakthrough times are in the order of hundred thousand years. At dam sites, however, where the length of fractures through which water flows from the input at the bottom of the impounded lake to its output are in the order of several hundred meters and hydraulic heads are high, these times are reduced by several orders of magnitude.

Recent modeling approaches on two-dimensional domains of dam sites have shown that under unfavorable conditions, leakage below dam sites can increase to an unbearable extent within the lifetime of the structure. How does inefficient sealing of fractures in the region of the grouting curtain influence leakage?

Modeling concept

Figure 1 presents a two-dimensional section of a dam site. The modeling domain is 750 m × 375 m × 1 m,

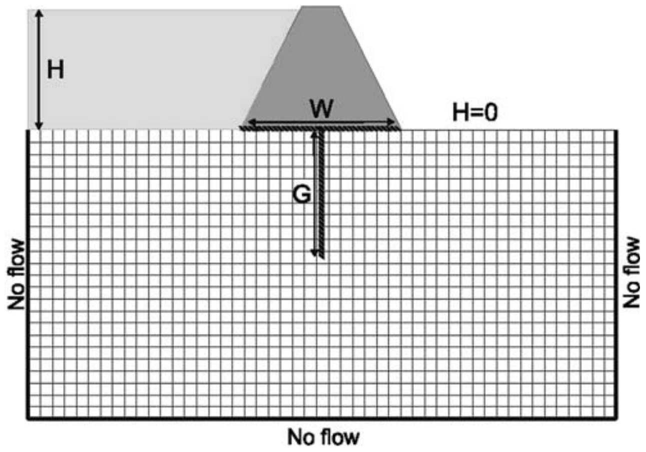

Fig. 1 Modeling domain of a dam site

divided by fractures into blocks of 7.5 m × 7.5 m × 1 m. To each of these fractures an individual aperture width can be assigned. The regions sealed by grouting are modeled by assigning aperture widths of 0.002 cm. The sealing apron has a width $W = 82$ m and the grouting curtain reaches down to depth $G = 187.5$ m.

All other regions of the domain carry fractures with aperture widths $a_0 = 0.02$ cm. The bottom of the domain, its upstream and downstream boundaries and the dam itself are impermeable. Water is impounded to a height of $H = 150$ m on the upstream side of the dam. To model the evolution of the fracture aperture widths in the first step, the flow rates through all fractures are calculated using fluid dynamics of laminar or turbulent flow. Next, the concentrations of dissolved calcium are obtained by use of the dissolution rates (2). From these, widening of each fracture during a time step Δt is found. For this new net of fractures the procedure described above is iterated until user defined, unbearable leakage rates are obtained. The following chemical parameters, characteristic for limestone, are used: $n = 4$; $k_n = 4 \times 10^{-8}$ mol cm^{-2} s^{-1}, $c_{eq} = 2 \times 10^{-6}$ mol cm^{-3}. The input concentration of the water is $c_{in} = 0$. Details are given by Romanov et al. (2003) and by Romanov (2003).

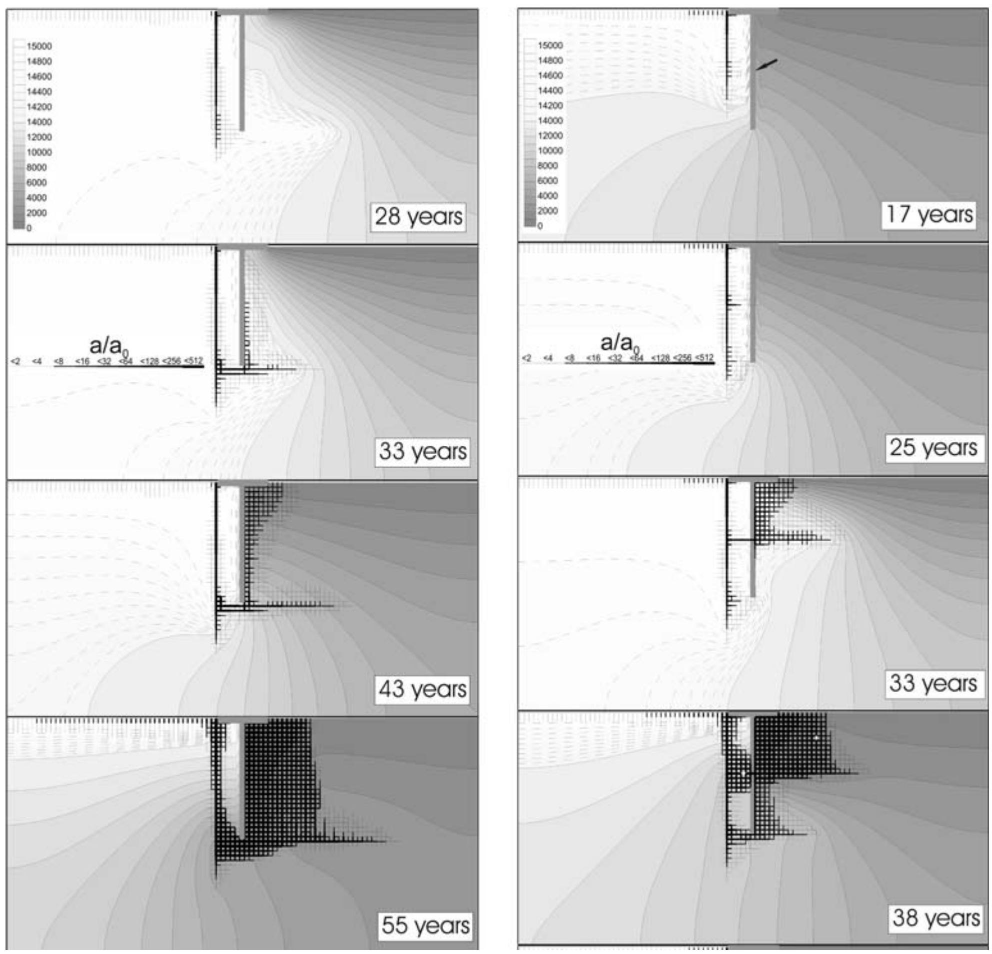

Fig. 2 Evolution of fracture aperture widths for scenarios A and B. $a_g = 0.002$ cm, $a_0 = 0.02$ cm. The aperture widths are given by the bar code in multiples of 0.02 cm. For better visualization all fractures with aperture widths less than 0.022 cm are omitted. Isolines of head are given in distances of 1 m (*dashed*) and 10 m (*full lines*). The values for the grey scale are in centimetres

Results

The following model runs are presented in this work: scenario A (Fig. 2): grouting is perfect and exhibits low permeability with fracture aperture widths a_g = 0.002 cm down to a depth of 187.5 m. In scenarios B and C deficiency of grouting leaves one unsealed fracture through the grouting curtain. In scenario C this fracture is located at a depth of 22.5 m in the upper part of the grouting curtain, whereas in scenario B the unsealed fracture is at a depth of 97.5 m in its center part. Finally, in scenario D the unsealed fracture is located at a depth of 165 m, close to the base of the grouting curtain (Fig. 3).

The fracture aperture widths at selected times are presented by a bar code. Distribution of hydraulic heads by isolines of head are also shown. Figure 4 shows the evolution of total leakage of the dam for scenarios A, B, and C.

Figure 2A shows the evolution of scenario A. After 28 years a vertical channel parallel to the grouting has propagated down to the end of the grouting curtain. At the tip of this channel the hydraulic head is almost equal to the head of 150 m imposed by the height of the impounded water. Flow is directed parallel below the grouting and then upwards to the surface at the valley downstream.

This can be visualized from the isolines of head to which flow is perpendicular. Some small channels have already migrated downhead below the grouting. After 33 years these channels have migrated further towards the exit. Because of the high gradients parallel to the grouting, vertical channels have reached the surface downstream after 43 years. At that time breakthrough occurs and the flow rates increase dramatically. From then on flow becomes turbulent and an integrated net of channels reaching the surface is created (55 years). The current model domain represents a section of 1 m width. Therefore, the leakage is given in $cm^3\ s^{-1}$ per 1 m width of the dam. For a dam site 100 m wide, a flow rate of $2 \times 10^5\ cm^3\ s^{-1}$ per 1 m width, amounts to a leakage of $20\ m^3\ s^{-1}$, which can be assumed as unbearable. After only 50 years the model dam site has failed. It must be noted, however, that the breakthrough times for dam

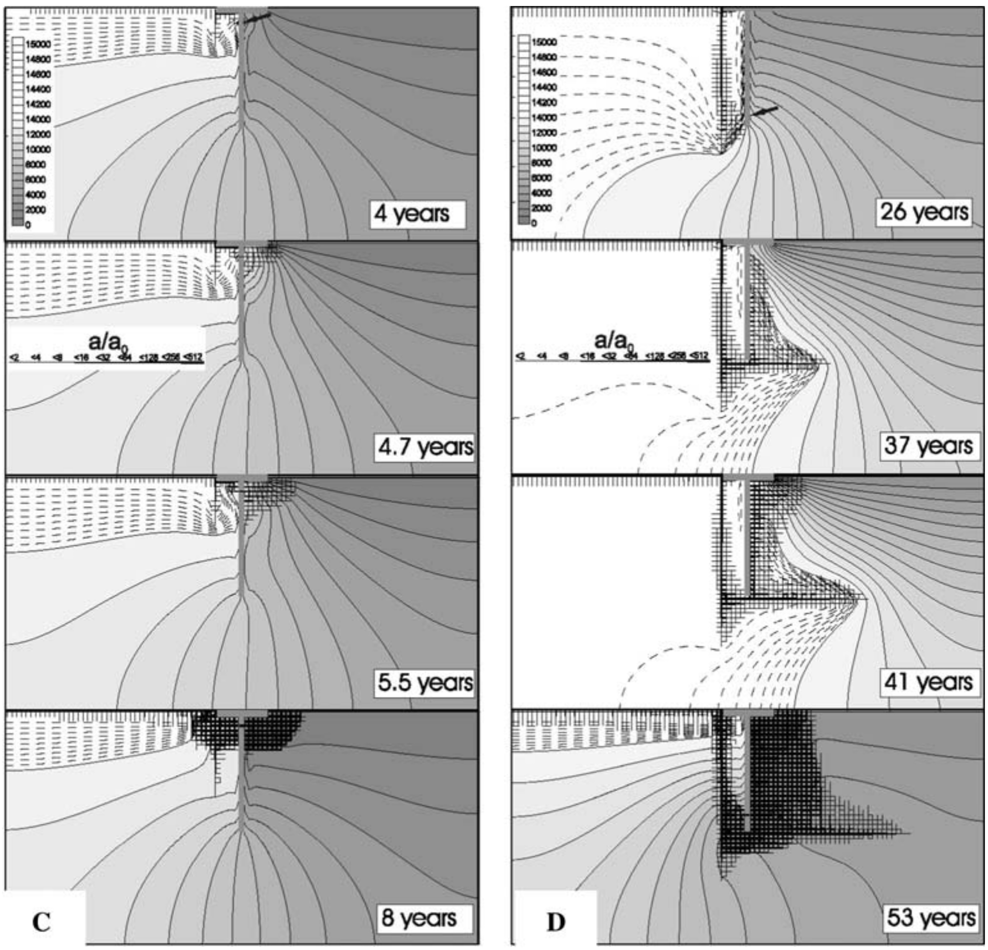

Fig. 3 Evolution of fracture aperture widths for scenarios C and D

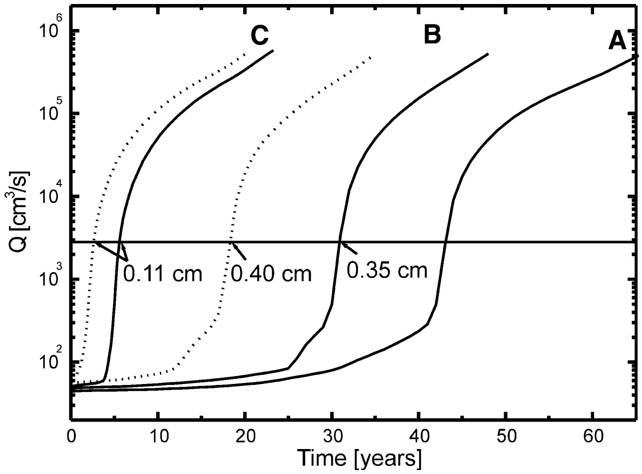

Fig. 4 Evolution of leakage for 1 m of dam with perfect grouting (A), and scenarios B and C depict aperture width of the unsealed fracture of 0.01 cm; the dotted lines stand for aperture width of 0.02 cm. The numbers on the curves give the aperture width of the unsealed fracture at breakthrough

sites show a similar power law as that of a single fracture (Eq. 1), (Romanov et al. 2003; Romanov 2003). Therefore, a reduction of the fracture aperture widths a_0 to 0.01 cm increases breakthrough time by a factor of 8, and the model dam site with aperture width $a_0 < 0.01$ cm can be regarded as safe. On the other hand, deeper grouting will also increase breakthrough time. Figure 2B shows the evolution of scenario B, where insufficient grouting leaves an unsealed fracture of 0.01 cm aperture width at a location of 97.5 m below ground. In the beginning, as in scenario A, a vertical channel propagates downwards (17 years). After 25 years it has reached the base of the grouting curtain and channels parallel to the surface start to migrate below the grouting. At the same time the unsealed fracture attracts flow and becomes enlarged. After 33 years this channel has been successful in the competition for breakthrough and most of the leakage flow is transported through it. Breakthrough time is reduced to 33 years in comparison to 43 years in scenario A.

Figure 4 shows the evolution of flow rates. If the fracture through the grouting has an aperture width of 0.02 cm, breakthrough time is reduced to 19 years. This is also shown in Fig. 4 by the dotted line.

In scenario C it is assumed that insufficient grouting leaves an open fracture with aperture width of 0.01 cm at 22.5 m below ground. The evolution is shown in Fig. 3. After 4 years a channel propagates downwards, but at the same time flow is attracted by the open fracture and dissolution creates a horizontal channel below the sealing apron. After 4.7 years this channel has joined the open fracture and breakthrough through it occurs after only 5.5 years. Then an integrated net of widened fractures is created and all leakage flows through the unsealed fracture. If the initial aperture width is assumed to be 0.02 cm, breakthrough occurs almost immediately after only 1 year. The evolution of flow rates for both cases is shown in Fig. 4. Finally, scenario D has been modeled with one open fracture with aperture width of 0.01 cm 165 m below ground. Figure 3D shows the evolution. It is very similar to scenario A. Some flow is attracted by the open fracture but the alternative pathways below the grouting turn out to be more competitive and breakthrough occurs after 41 years.

Conclusion

From these results the reduction of breakthrough times by inefficiencies in grouting is concluded to be the more severe the closer the unsealed fractures are to the sealing apron. In other words, this inefficiency of grouting reduces the efficiency of the grouting curtain below the unsealed fractures. For comparison, breakthrough times are calculated for dam sites with perfect grouting, but with a reduced grouting depth G of 22.5, 97.5, and 167.5 m. These are 3, 17, and 33 years, respectively. The reduction of breakthrough times also depends on the aperture width of the unsealed fractures. For completely unsealed fractures of aperture width $a_0 = 0.02$ cm breakthrough times are almost identical to those of perfectly grouted dams with curtains reaching down to the depth where the unsealed fracture is located. Partial sealing to aperture widths of 0.01 cm increases breakthrough times.

One final comment must be given; the inefficiencies in grouting generally will not occur along the entire width of the dam. If the grouting fails along a width V, its contribution to leakage is $V\,Q_i(t)$, where $Q_i(t)$ is the leakage per meter at time t and can be read from the corresponding curve in Fig. 4. The total leakage is $Q_{tot}(t) = Q_g(t)(U - V) + Q_i(t)V$. U is the total width of the dam and $Q_g(t)$ the leakage of a dam with perfect grouting.

References

Dreybrodt W (1996) Principles of early development of karst conduits under natural and man-made conditions revealed by mathematical analysis of numerical models. Water Resour Res 32(9):2923–2935

Dreybrodt W, Gabrovsek F (2003) Basic processes and mechanisms governing the evolution of karst. In: Speleogenesis and evolution of karst aquifers, vol 1(1). www.speleogenesis.info, 26 pp. Republished from: Gabrovsek F (ed) (2002) Evolution of karst: from prekarst to cessation. Postojna-Ljubljana, Zalozba ZRC, pp 115–154

Eisenlohr L, Meteva K, Gabrovsek F, Dreybrodt W (1999) The inhibiting action of intrinsic impurities in natural calcium carbonate minerals to their dissolution kinetics in aqueous H_2O–CO_2 solutions. Geochim Cosmochim Acta 63(7–8):989–1001

Jeschke AA, Vosbeck K, Dreybrodt W (2001) Surface controlled dissolution rates of gypsum in aqueous solutions exhibit nonlinear dissolution kinetics. Geochim Cosmochim Acta 65(1):27–34

Romanov D (2003) Evolution of karst aquifers in natural and man made environments: a modeling approach, Bremen

Romanov D, Gabrovsek F, Dreybrodt W (2003) Dam sites in soluble rock: a model of increasing leakage by dissolutional widening of fractures beneath a dam. Eng Geol 70(1–2):17–35